Acta Crystallographica Section B
Structural Science
ISSN 0108-7681

In situ high-pressure crystallization and compression of halogen contacts in dichloromethane

Marcin Podsiadło, Kamil Dziubek and Andrzej Katrusiak*

Faculty of Chemistry, Adam Mickiewicz University, Grunwaldzka 6, 60-780 Poznań, Poland

Correspondence e-mail: katran@amu.edu.pl

Received 20 May 2005
Accepted 2 June 2005

The structure of dichloromethane, CH_2Cl_2, crystallized *in situ* in a diamond–anvil cell, has been determined by single-crystal X-ray diffraction at 1.33 and 1.63 GPa. The pressure-frozen crystal was determined to be orthorhombic, with the space group *Pbcn*, and isostructural with the low-temperature phase at 0.1 MPa. The CH_2Cl_2 molecules are located on one set of crystallographic twofold axes. The characteristics determined for the CH_2Cl_2 crystal (compression of the close intermolecular contacts, molecular association and the crystal habit of dichloromethane) suggest that the crystal cohesion forces are dominated by H···Cl interactions rather than by Cl···Cl attractions.

1. Introduction

Dichloromethane is one of the simplest alkyl halides; it was shown by Raman (Shimizu, 1984) and FT IR (Shimizu *et al.*, 1984) spectroscopies to undergo a phase transition at *ca* 4.5 GPa. Thus, it is a convenient compound for studying monotonic structural transformations and intermolecular halogen···halogen interactions in molecular crystals below this pressure. Most recently we determined the crystal structures of 1,2-dichloroethane (Bujak *et al.*, 2004) and 1,1,2,2-tetrachloroethane (Bujak & Katrusiak, 2004). The pressure-frozen structure of 1,2-dichloroethane is isostructural with the α-phase crystallized by cooling (Boese *et al.*, 1992), while a new phase has been observed for pressure-frozen 1,1,2,2-tetrachloroethane (Bujak & Katrusiak, 2004). Both these high-pressure structures of ethane derivatives are disordered and the Cl···Cl interactions clearly change when the 1,2-dichloroethane transforms between phases α and β. The Cl···Cl contacts are often regarded as energetically weaker than hydrogen bonds, but stronger than van der Waals interactions. They are thought to play an important role in molecular arrangement in crystals (Legon, 1999; Metrangolo & Resnati, 2001). There is also an alternative hypothesis that the occurrence of short Cl···Cl distances results from the so-called *chlorophobic effect* (Grineva & Zorky, 1998, 2000), in which the molecules arrange themselves in order to minimize the number of contacts between the Cl atoms and atoms of other types. The suggestion of this effect was based on the observation made for aromatic chloro derivatives that interactions with Cl atoms are the least favourable (least attractive). Hence, the Cl···Cl contacts are formed as a mere consequence of other molecular fragments aggregating together. The main purpose of the present study is to investigate the hierarchy of intermolecular interactions in CH_2Cl_2 and to compare these interactions with those in 1,2-dichloro- and 1,1,2,2-tetrachloroethane. The dichloromethane molecule is small, rigid and does not undergo conformational transfor-

Table 1
Crystal data and details of the refinements of CH_2Cl_2 at 1.33 (5) GPa/293.0 (5) K and 1.63 (5) GPa/293.0 (5) K.

	1.33 GPa	1.63 GPa
Crystal data		
Chemical formula	CH_2Cl_2	CH_2Cl_2
M_r	84.93	84.93
Cell setting, space group	Orthorhombic, *Pbcn*	Orthorhombic, *Pbcn*
a, b, c (Å)	3.984 (1), 7.863 (2), 9.357 (2)	3.924 (1), 7.793 (2), 9.335 (2)
V (Å^3)	293.12 (12)	285.46 (12)
Z	4	4
D_x (Mg m^{-3})	1.920	1.972
Radiation type	Mo $K\alpha$	Mo $K\alpha$
No. of reflections for cell parameters	1459	1495
θ range (°)	5–30	5–30
μ (mm^{-1})	1.86	1.91
Temperature (K)	293 (2)	293 (2)
Crystal form, colour	Cylinder, colourless	Cylinder, colourless
Crystal size (mm)	0.42 × 0.42 × 0.14	0.42 × 0.42 × 0.14
Data collection		
Diffractometer	Kuma KM4CCD κ geometry	Kuma KM4CCD κ geometry
Data collection method	ω scans	ω scans
DAC absorption and gasket shadowing correction	Analytical	Analytical
T_{min}	0.50	0.46
T_{max}	0.85	0.86
No. of measured, independent and observed reflections	2203, 219, 188	2063, 174, 157
Criterion for observed reflections	$I > 2\sigma(I)$	$I > 2\sigma(I)$
R_{int}	0.096	0.068
θ_{max} (°)	29.6	29.9
Range of h, k, l	$-5 \Rightarrow h \Rightarrow 5$ $-10 \Rightarrow k \Rightarrow 10$ $-5 \Rightarrow l \Rightarrow 5$	$-5 \Rightarrow h \Rightarrow 5$ $-10 \Rightarrow k \Rightarrow 10$ $-4 \Rightarrow l \Rightarrow 4$
Refinement		
Refinement on	F^2	F^2
$R[F^2 > 2\sigma(F^2)]$, $wR(F^2)$, S	0.061, 0.190, 1.28	0.055, 0.135, 1.25
No. of reflections	219	174
No. of parameters	20	19
H-atom treatment	Mixture of independent and constrained refinement	Mixture of independent and constrained refinement
Weighting scheme	$w = 1/[\sigma^2(F_o^2) + (0.1099P)^2 + 0.0415P]$, where $P = (F_o^2 + 2F_c^2)/3$	$w = 1/[\sigma^2(F_o^2) + (0.0601P)^2 + 0.5145P]$, where $P = (F_o^2 + 2F_c^2)/3$
$(\Delta/\sigma)_{max}$	<0.0001	<0.0001
$\Delta\rho_{max}$, $\Delta\rho_{min}$ (e Å^{-3})	0.29, −0.28	0.29, −0.28
Extinction method	*SHELXL*	None
Extinction coefficient	0.11 (4)	–

Computer programs used: *CrysAlis* (Oxford Diffraction, 2004), *SHELXS*97 (Sheldrick, 1997), *SHELXL*97 (Sheldrick, 1997), *XP* (Siemens, 1990).

mations. High pressure can efficiently modify the structure of the molecular crystals, which can be efficiently monitored by diffraction studies. High pressure was successfully applied to resolve the role of hydrogen bonds in structural phase transitions (Katrusiak, 1996, 2001, 2004*a*). A reverse effect – of transforming hydrogen bonds introducing structural strain – was also documented for crystals under various thermodynamic conditions (Katrusiak, 1993). High pressure was also employed to reveal the role of intermolecular forces on the molecular association in crystal structures of biologically important compounds, such as peptides (Boldyreva *et al.*, 2003, 2005) and pharmaceutical drugs (Boldyreva *et al.*, 2000; Boldyreva, 2004). However, relatively few simple organic compounds have been studied at high pressure and no general reference data on the compression of intermolecular contacts in such compounds is available. It was hoped that the comparison of its low-temperature and high-pressure structures would contribute to a better understanding of the Cl···Cl interactions and their role in molecular arrangement in the dichloromethane crystal.

2. Experimental

Dichloromethane (m.p. 176 K; analytical grade from POCh) was used without further purification. It was loaded into a four-pin diamond–anvil cell (DAC) sealed with a 0.3 mm thick steel gasket. The pressure calibration gave 1.33 (5) GPa at 298 K when the compound froze as a polycrystal, filling the volume of the high-pressure chamber. This pressure was only slightly higher than the freezing pressure of 1.25 GPa which was estimated to be the average of both Bridgman's measurements (Bridgman, 1942, 1949). The freezing pressure determined by Shimizu (1984) and Shimizu *et al.* (1984) was even lower (1.13 GPa). The slight differences between these values may be due to the different temperatures of the measurements. In our measurements, the pressure was calibrated by the ruby fluorescence method (Piermarini *et al.*, 1975) with a BETSA PRL spectrometer with an accuracy of 0.05 GPa, before and after the diffraction measurement. The DAC was heated, using a hot-air gun, to *ca* 363 K until all the crystal grains, except one, were melted. The DAC was then slowly cooled and the single crystal grew to fill the whole volume of the chamber. The gasket indented with the diamond culets was 0.14 mm thick and the spark-eroded hole had a diameter of 0.42 mm (dimensions of the single crystal). After collecting the diffraction data, the single crystal was heated to *ca* 413 K when the sample crystal melted until a fragment filling *ca* 5% of the volume of the chamber was left. The chamber volume was then reduced, after which the DAC was slowly cooled to room temperature. The pressure in the cell was 1.63 (5) GPa and this sample crystal was used for the next diffraction measurement. The single-crystal data collections were performed using a KM-4 CCD diffractometer with graphite-

Table 2
The molecular geometry and intermolecular distances in the low-temperature and high-pressure CH_2Cl_2 structures.

	153 K/0.1 MPa[a]	293 K/1.33 GPa [b]	293 K/1.63 GPa[b]
C—H (Å)	0.99 (13)	1.01 (9)	1.13 (12)
C—Cl (Å)	1.768 (13)	1.765 (4)	1.769 (5)
C···Cl (Å)[i]	3.492	3.360 (3)	3.324 (5)
Cl···Cl (Å)	2.932 (4)	2.919 (5)	2.922 (7)
$\angle\varphi$ (°)	32.3 (1)	31.07 (7)	30.76 (9)
∠Cl—C—Cl (°)	112 (1)	111.6 (3)	111.4 (4)

Symmetry code: (i) $\frac{1}{2}+x, \frac{1}{2}-y, -z$ and $-\frac{1}{2}+x, \frac{1}{2}-y, -z$. References: (*a*) Kawaguchi *et al.* (1973); (*b*) this work.

monochromated Mo $K\alpha$ radiation at 1.33 (5) and 1.63 (5) GPa, both at 293.0 (5) K. The gasket-shadow method (Budzianowski & Katrusiak, 2004) was applied to centre the DAC. The images were recorded using the ω-scan technique with 0.9° rotations and 40 s exposures (Budzianowski & Katrusiak, 2004). The *CrysAlisCCD* and *CrysAlisRED* programs (Oxford Diffraction, 2004) were used for data collection, determination of the *UB* matrix, and the initial data reduction and *Lp* corrections for both data sets. The reflection intensities have been corrected for the effect of absorption of X-rays by the DAC and the shadowing of the beams by the gasket edges (Katrusiak, 2003, 2004*b*). The unit-cell dimensions have been corrected for the effect of reflection-profile shifts due to crystal absorption and gasket shadowing (Katrusiak, 2004*c*). The structure was easily solved by direct methods using the program *SHELXS*97, and refined with atoms C1 and Cl1 being anisotropic by the program *SHELXL*97 (Sheldrick, 1997). The H atom was located in a difference-Fourier map and refined freely with an isotropic displacement parameter. Selected details of the structure refinements and crystal data are listed in Table 1. The final atomic parameters have been deposited.[1]

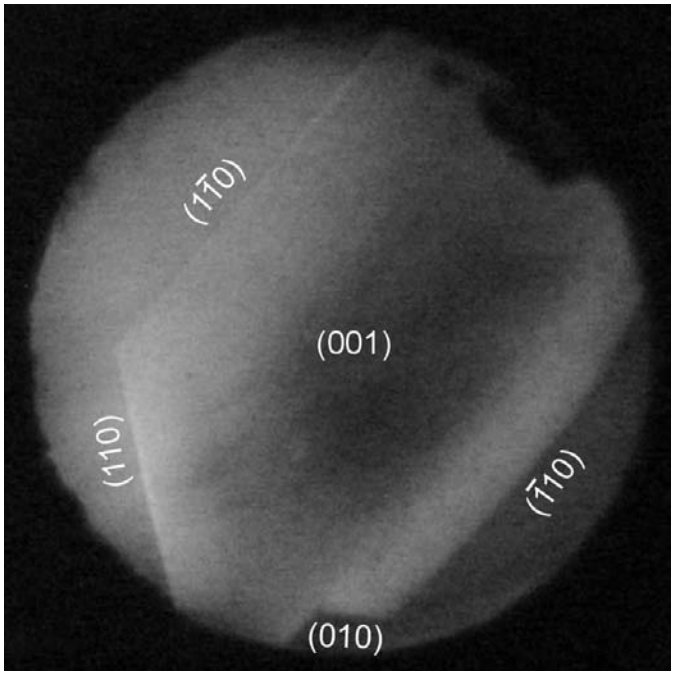

Figure 1
A single crystal of CH_2Cl_2 immediately after nucleation in the high-pressure chamber at 1.33 GPa – a very thin plate perpendicular to the viewing direction and close to the upper diamond culet. A ruby chip for pressure calibration is visible at the upper right edge of the chamber. The angle between the (110) and (1$\bar{1}$0) faces is 126.26°. The diameter of the high-pressure chamber is 0.42 mm.

3. Discussion

3.1. *In-situ* pressure crystallization

The pressure-frozen CH_2Cl_2 repeatedly crystallized as a very thin plate parallel to and close to the upper diamond culet (*cf.* Fig. 1). The appearance of the crystal plate on the upper culet may be accidental, due to the nucleation of the crystal. It quickly covered the culet surface and then grew slowly towards the lower culet. During the course of further crystallization aimed at obtaining a high-quality single crystal, the crystal [*z*] axis perpendicular to the plate – initially parallel to the DAC axis – changed its direction by *ca* 17°. Brown *et al.* (1969) investigated pressure-crystallized single crystals of CH_2Cl_2 by analysing their polarized IR and Raman spectra. They concluded that the CH_2Cl_2 molecules occupied C_2 (Hermann–Mauguin symbol: 2) sites. The birefringence measurements for the crystals grown along the crystallographic axes, as well as the observation of an angle of 120–125° between two crystal faces, led Brown *et al.* (1969) to the conclusion that the crystal is hexagonal, with D_{3h} ($\bar{6}m2$) symmetry. However, according to our observation, the obvious interfacial angle of *ca* 125° in the CH_2Cl_2 crystal plate is that between (110) and (1$\bar{1}$0) faces (see Fig. 1). The exact calculation of this angle, based on the unit-cell dimensions, gave a value of 126.26°.

The pressure-frozen CH_2Cl_2 crystal is isostructural with the crystal frozen at low temperature (Kawaguchi *et al.*, 1973). The crystal is anisotropic, with linear compressibility coefficients calculated between 1.33 and 1.63 GPa of: $\beta_a = -0.050$ GPa^{-1}, $\beta_b = -0.030$ GPa^{-1} and $\beta_c = -0.008$ GPa^{-1}. The compressibility of the crystal reflects the anisotropic character of the interactions and the molecular arrangement. This structure can be regarded as being built of layers perpendicular to [001] with each layer being composed of chains along [010]. Within each chain the molecules are arranged head-to-tail, with the shortest H···Cl contacts and most favoured electrostatic interactions of the molecular dipoles. The electrostatic interactions are unfavourable for the parallel arrangement of the chains within the layer. The least compressible direction, along the [001] axis perpendicular to the layers of molecules, corresponds to the shortest Cl···Cl contacts, while the crystal is stronger compressed along [100] and [010]. The intermolecular interactions within the layers are dominated by H···Cl contacts (see Fig. 2). The least compressible direction along [001] coincides with the direction of the slowest rate of

[1] Supplementary data for this paper are available from the IUCr electronic archives (Reference: AV5039). Services for accessing these data are described at the back of the journal.

crystal growth (perpendicular to the CH_2Cl_2 plate and parallel to the DAC axis, as shown in Fig. 1).

3.2. Molecular volume

The compression of the CH_2Cl_2 unit-cell volume at 1.33 and 1.66 GPa agrees well with the previous results obtained by Bridgman (1942, 1949). The measurements above 0.5 GPa were conducted with piston-seal arrangements (Bridgman, 1942, 1949) and with a supplementary piston and cylinder apparatus (Bridgman, 1949) below 0.5 GPa. Based on the our results and those obtained by Bridgman (1942) the relative volume change of fusion is given as $\Delta V_f/V = 0.054$ at 293 K (Fig. 3). Such a significant density jump when the liquid freezes under isochoric conditions considerably reduces the pressure and usually leads to an equilibrium between the liquid and crystalline states in the high-pressure chamber. This liquid–solid equilibrium in the chamber may handicap the diffraction studies and should be avoided if possible. On the other hand, the anisotropic samples fully filling the chamber may be subjected to some strain due to the temperature changes.

3.3. Intermolecular interactions

The CH_2Cl_2 molecules are located on one set of crystallographic twofold axes, as shown in Fig. 2. In both high-pressure structures the shortest intermolecular Cl···Cl distances (Table 2) are shorter than the sum of the van der Waals radii of two Cl atoms, 3.6 Å (Batsanov, 2001; Kitaigorodskii, 1973; Nyburg & Faerman, 1985). The Cl···Cl intermolecular interactions – if stronger than the van der Waals forces involving other atoms – should be the least compressed (*i.e.* the stiffest) contacts in the crystal structure. The differentiation of the energy of intermolecular forces should also be reflected in the molecular packing, the crystal habit and the unit-cell compression. Generally, the compression of contacts provides information on the derivative of the energy of interactions with respect to distance, $\partial E/\partial r$. The magnitude of this derivative is usually larger for stronger (more energetic) interactions than for weaker ones, however, also for weak interactions [with shallow $E(r)$ minimum] the shortening of distances may result in a steep rise in energy. Moreover, despite the relatively simple molecular structure of CH_2Cl_2 the cohesion forces in this crystal cannot be easily classified. For example, it appears that the molecules along [001] interact *via* Cl···Cl contacts (the lengths of which are commensurate with the sum of the van der Waals radii), however, these molecules are also attracted electrostatically owing to the net atomic charges of Cl and H atoms (*cf.* Fig. 2).

The molecular dimensions determined for the high-pressure structure agree very well with those determined at 0.1 MPa/153 K (Kawaguchi *et al.*, 1973), and the molecules can be regarded as being rigid, within experimental error. The intermolecular distances and molecular geometry of low-temperature and high-pressure structures are compared in Table 2; the high-pressure structural dimensions are illustrated in Fig. 2. There are two types of intermolecular contacts commensurate with the sum of the van der Waals radii of the atoms: H···Cl and Cl···Cl, of 3.0 and 3.6 Å, respectively. The shortest H···Cl and Cl···Cl contacts compress at a similar rate (Fig. 4). It can be observed from Fig. 2 that the compression of the CH_2Cl_2 structure may be analysed in terms of the squeezed intermolecular contacts and molecular rotations about the twofold axes. The orientation of the CH_2Cl_2 molecule can be conveniently described by the φ angle between the [***z***] axis and the projection of the C—Cl bond on the ***xz*** plane (Kawaguchi *et al.*, 1973), as shown in Fig. 2. In principle, if the Cl···Cl and H···Cl contacts are at the stable position (*i.e.* $\partial E/\partial r = 0$) and there are no voids in the CH_2Cl_2 structure at 0.1 MPa, the pressure dependence of the φ angle should indicate which of these contacts is stiffer. According to this reasoning, the molecular rotations should relax the unevenly distributed strains in the intermolecular contacts, which are generated in the compressed crystal. However, in the CH_2Cl_2 structure, the distribution of the closest contacts is quite complex (Fig. 2) and it does not simply allow the H···Cl and Cl···Cl forces to decompose into those favouring the opening or closing angle φ. It is evident from Fig. 4 that $\partial\varphi/\partial p$ is negative and that the molecules rotate in such a way

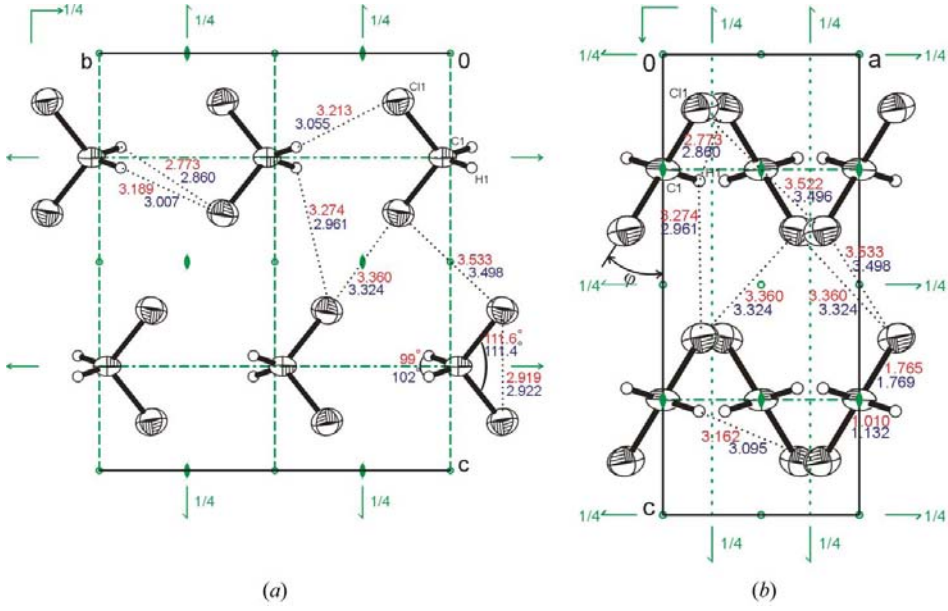

Figure 2
Selected molecular dimensions and short intermolecular distances (Å) are indicated for the structure compressed to 1.33 (5) GPa (red) and 1.63 (5) GPa (blue). The displacement ellipsoids are shown at the 50% probability level.

that reduces the compression of the crystal along [001], which is reflected in the smallest magnitude of β_c.

The crystal habit can also be employed in the analysis of intermolecular forces. The speed of the crystal growth can be interpreted as a derivative of the intermolecular interactions in the structure. It can be inferred that the quickest rate of crystal growth proceeds in the direction where the molecular interactions are the strongest, while the slowest rate of the crystal growth is in the direction of the weakest attraction between the molecules. It would indicate that the molecular attraction is the strongest along the ***xy*** plane where the molecular interactions are dominated by H···Cl contacts. A much slower rate of crystal growth was observed along [001], where exclusively short Cl···Cl contacts are present. This observation on its own would suggest that the Cl···Cl attraction is weaker than H···Cl, however, this reasoning neglects all other cohesion forces, *e.g.* electrostatic interactions of the polar CH_2Cl_2 molecules.

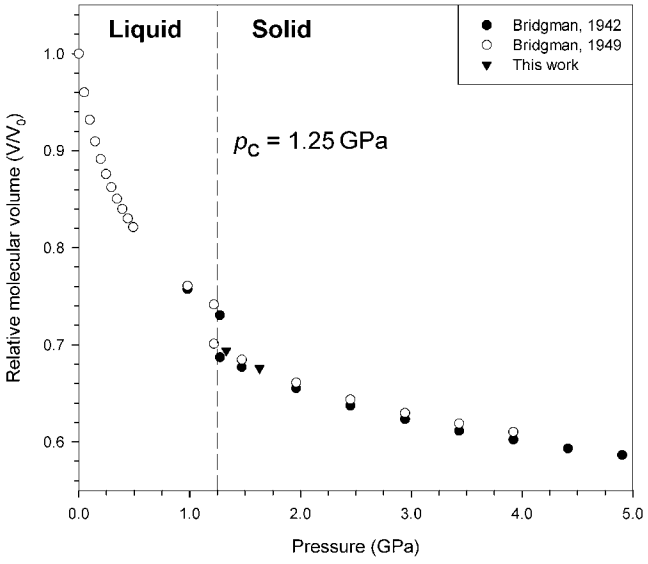

Figure 3
Relative changes of the molecular volume of CH_2Cl_2 at 298 K determined in this work (triangles) and those measured by Bridgman (1942, 1949).

The shortest Cl···Cl intermolecular interactions observed in the pressure-frozen 1,1,2,2-tetrachloroethane at 0.5 GPa (Bujak & Katrusiak, 2004), and in 1,2-dichloroethane at 0.7 GPa (α-phase; Bujak *et al.*, 2004), are 3.478 and 3.587 Å, respectively. There are three close Cl···Cl intermolecular contacts (shorter than the sum of the van der Waals radii) to each independent Cl atom in the CH_2Cl_2 structure, to one Cl atom in 1,2-dichloroethane, while in 1,1,2,2-tetrachloroethane one of the independent Cl atoms has two such close neighbours and the other Cl atom only one. Thus, the number of close Cl···Cl contacts appears to be correlated with the contents of the Cl atoms in the compound, which may be an indication that the number of Cl···Cl contacts is a more 'statistical' feature than an energetic property resulting from Cl···Cl forces being significantly stronger than other van der Waals interactions.

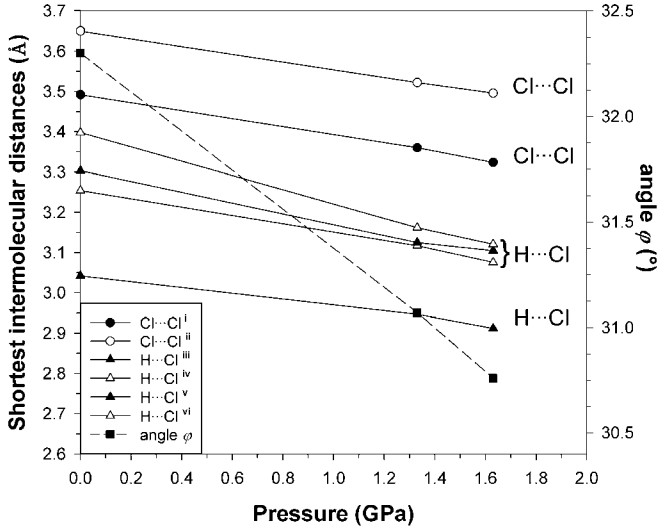

Figure 4
The shortest intermolecular contacts and molecular rotation angle φ as a function of pressure in the 0.1 MPa/153 K (Kawaguchi *et al.*, 1973), 1.33 GPa/293 K and 1.63 GPa/293 K structures. The lines joining the points have been drawn only as a guide to the eye. Since the precision of the H-atom position refined from the X-ray diffraction data is lower than that of heavy atoms, the more reliable H atoms ideally located from the molecular geometry (d_{C-H} = 0.97 Å) have been used to calculate the intermolecular contacts. The symmetry codes are: (i) $-\frac{1}{2}+x, \frac{1}{2}-y, -z$ and $\frac{1}{2}+x, \frac{1}{2}-y, -z$; (ii) $1-x, y, \frac{1}{2}-z$; (iii) $\frac{1}{2}-x, -\frac{1}{2}+y, z$; (iv) $1-x, y, \frac{1}{2}-z$; (v) $x, -y, \frac{1}{2}+z$; (vi) $-\frac{1}{2}+x, -\frac{1}{2}+y, \frac{1}{2}-z$.

4. Conclusions

The pressure dependence of the CH_2Cl_2 structure has been determined at 1.33 and 1.63 GPa. However, the compression of the Cl···Cl and H···Cl intermolecular contacts, their distribution and directions relative to the crystal habit is not conclusive with respect to the role of Cl···Cl forces in the formation of crystals. On the other hand, the compressibility of the crystal structure shows that the Cl···Cl and H···Cl contacts are squeezed at a similar rate (Fig. 4). Consideration of the crystal habit and its rate of growth, and an inspection of the molecular arrangement indicates that the strongest intermolecular interactions are within the layers perpendicular to [001]. These observations can be interpreted as consistent with the existence of the chlorophobic effect postulated by Grineva & Zorky (1998, 2000). Therefore, further studies on the structure of compounds with very weakly interacting molecules need to be carried out to resolve the role of halogen···halogen interactions in the formation of crystals.

This study was supported by the Polish Ministry of Scientific Research and Information Technology, Grant No. 3-T09A18127.

References

Batsanov, S. S. (2001). *Inorg. Mater.* **37**, 871–885.

Boese, R., Bläser, D. & Haumann, T. (1992). *Z. Kristallogr.* **198**, 311–312.

Boldyreva, E. V. (2004). *High-Pressure Crystallography*, edited by A. Katrusiak & P. F. McMillan, pp. 495–512. Dordrecht: Kluwer Academic Publishers.

Boldyreva, E. V., Ahsbahs, H. & Weber, H.-P. (2003). *Z. Kristallogr.* **218**, 231–236.

Boldyreva, E. V., Ivashevskaya, S. N., Sowa, H., Ahsbahs, H. & Weber, H.-P. (2005). *Z. Kristallogr.* **220**, 50–57.

Boldyreva, E. V., Shakhtshneider, T. P., Vasilichenko, M. A., Ahsbahs, H. & Uchtmann, H. (2000). *Acta Cryst.* B**56**, 299–309.

Bridgman, P. W. (1942). *J. Chem. Phys.* **9**, 794–797.

Bridgman, P. W. (1949). *Proc. Am. Acad. Arts. Sci.* **77**, 129–146.

Brown, C. W., Obremski, R. J., Allkins, J. R. & Lippincott, E. R. (1969). *J. Chem. Phys.* **51**, 1376–1384.

Budzianowski, A. & Katrusiak, A. (2004). *High-Pressure Crystallography*, edited by A. Katrusiak & P. F. McMillan, pp. 101–112. Dordrecht: Kluwer Academic Publishers.

Bujak, M., Budzianowski, A. & Katrusiak, A. (2004). *Z. Kristallogr.* **219**, 573–579.

Bujak, M. & Katrusiak, A. (2004). *Z. Kristallogr.* **219**, 669–674.

Grineva, O. V. & Zorky, P. M. (1998). *Zh. Fiz. Khim.* **72**, 714–720 (in Russian).

Grineva, O. V. & Zorky, P. M. (2000). *Kristallografiya*, **45**, 692–698 (in Russian).

Katrusiak, A. (1993). *Phys. Rev. B*, **48**, 2992–3002.

Katrusiak, A. (1996). *Ferroelectrics*, **188**, 5–10.

Katrusiak, A. (2001). *Frontiers of High-Pressure Research*, edited by H. D. Hochheimer, B. Kuchta, P. K. Dorhout & J. L. Yarger, pp. 73–85. Dordrecht: Kluwer Academic Publishers.

Katrusiak, A. (2003). *REDSHADE.* Adam Mickiewicz University, Poznań.

Katrusiak, A. (2004*a*). *High-Pressure Crystallography*, edited by A. Katrusiak & P. F. McMillan, pp. 513–520. Dordrecht: Kluwer Academic Publishers.

Katrusiak, A. (2004*b*). *Z. Kristallogr.* **219**, 461–467.

Katrusiak, A. (2004*c*). *REDSHUB*. Adam Mickiewicz University, Poznań.

Kawaguchi, T., Tanaka, K., Takeuchi, T. & Watanabe, T. (1973). *Bull. Chem. Soc. Jpn*, **46**, 62–66.

Kitaigorodskii, A. I. (1973). *Molecular Crystals and Molecules.* New York: Academic Press.

Legon, A. C. (1999). *Angew. Chem. Int. Ed.* **38**, 2686–2714.

Metrangolo, P. & Resnati, G. (2001). *Chem. Eur. J.* **7**, 2511–2519.

Nyburg, S. C. & Faerman, C. H. (1985). *Acta Cryst.* B**41**, 274–279.

Oxford Diffraction (2004). *Xcalibur CCD* and *CrysAlis Software* Systems, Version 1.171. Oxford Diffraction Ltd, England.

Piermarini, G. J., Block, S., Barnett, J. D. & Forman, R. A. (1975). *J. Appl. Phys.* **46**, 2774–2780.

Sheldrick, G. M. (1997). *SHELXS*97 and *SHELXL*97. University of Göttingen, Germany.

Shimizu, H. (1984). *Chem. Phys. Lett.* **105**, 268–272.

Shimizu, H., Xu, J., Mao, H. K. & Bell, P. M. (1984). *Chem. Phys. Lett.* **105**, 273–276.

Siemens (1990). *XP*, Version 4.2. Siemens Analytical X-ray Instruments Inc., Madison, Wisconsin, USA.